Progress In Electromagnetics Research M, Vol. 92, 137–145, 2020

Formulation of THz Sensor Array Systems with Metamaterials

Brinta Chowdhury[1] and Abdullah Eroglu[1, 2, *]

Abstract—The complete analytical formulation of periodic structures using metamaterials formed with split ring resonators (SRRs) is developed. The periodic structure modeling is based on coplanar waveguide transmission line method and network parameters. The full effect of mutual inductances in the array design is integrated for the first time using curve fitting techniques with electromagnetic simulator. The simplified equivalent circuit including the effect of mutual inductance is presented. The proposed formulation is then used to design a unit cell composed of two SRRs of the sensor array. The analytical method is then verified with simulation results. The prototype of the unit cell has then been manufactured and measured at different frequencies. The analytical, simulation, and measurement results are compared, and agreement has been confirmed.

1. INTRODUCTION

Metamaterials are of a great interest due to their ability to present artificially custom material characteristics independent of the existing material characteristics at all frequency ranges. The concept of metamaterials was first introduced by Veselago in 1967 [1]. However, its realization was not possible until 1996 when emulation of continuous media with negative permittivity was demonstrated [2]. Open loop, conducting ring structures, called Split Ring Resonator (SRR), on a dielectric substrate were proposed and implemented to obtain negative permittivity [3]. Yen et al. demonstrated magnetic resonances for metamaterials in the THz range [4].

The introduction of thin wires with SRRs introduces backward wave propagation and demonstrates negative permittivity and permeability as experimented and shown by Smith et al. [5]. This helped evolvement of resonant type metamaterial transmission line structures consisting of co-planar waveguide (CPW) and SRRs. CPW is etched on one side of the dielectric substrate using transmission lines where SSR is placed on the other side. This creates a unit cell [6]. In the formed resonant structure, the transmission lines generate the negative permittivity whereas SRRs give the negative permeability in a narrow band above their resonance frequency. Metamaterial transmission lines get great attention due to their compact size and increased functionalities compared to regular transmission lines [7]. They are being used in many applications including stopband filters with a flexibility to control the bandwidth [8]. There have been several reports about the analysis of transmission lines with SRRs. The method in [9] uses equivalent lumped circuits to model SRR loaded coplanar waveguide (CPW) transmission lines.

In this paper, the complete analytical formulation for THz sensor arrays formed with SRRs and CPW transmission lines is given. The formulation is practical and uses network parameters with CPW principles. In the proposed method, the full effect of the mutual coupling in the resonant structure is taken into account. The analytical model is verified with 3D electromagnetic simulator. The prototype has been built and measured at different frequencies. It has been confirmed that analytical, simulated, and measured results are in agreement. The novelty of this work is the simplified formulation of SRR and estimation of the mutual inductance between SRR and CPW lines. To our best knowledge, there

Received 21 February 2020, Accepted 26 April 2020, Scheduled 11 May 2020
* Corresponding author: Abdullah Eroglu (aeroglu@ncat.edu).
[1] ECE Department, North Carolina A&T State University, USA. [2] ECE Department, Purdue University, Fort Wayne, USA.

is no literature found where mutual inductance is expressed as a function of physical dimensions. The proposed method can be used in several applications including the design of sensors for biomedical applications, tuning elements, and antennas at the THz range.

2. ANALYTICAL FORMULATION

The proposed structure is considered to be a unit cell formed with CPW transmission lines and SRRs with single gap. The CPW transmission lines are etched on one side, and SRR is implemented on the other side of the dielectric substrate as illustrated in Figure 1.

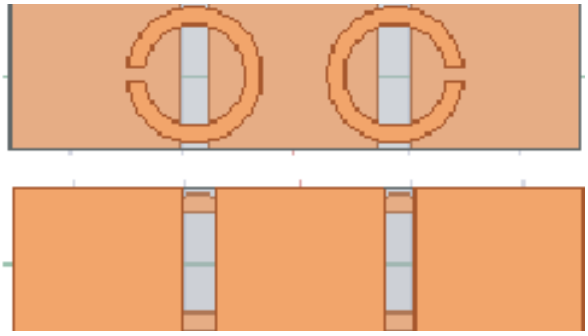

Figure 1. Unit cell formed with CPW transmission line and SRR.

2.1. Formulation of Coplanar Waveguide

The coplanar waveguide shown in Figure 2 can be represented by an equivalent lumped circuit shown in Figure 3 [6]. Per unit length inductance and capacitance values for the elements in Figure 3 can be obtained using the relations given by

$$L_{pul} = \frac{Z_o\sqrt{\varepsilon}_e}{c_o} \tag{1}$$

$$C_{pul} = \frac{\sqrt{\varepsilon}_e}{c_o Z_o} \tag{2}$$

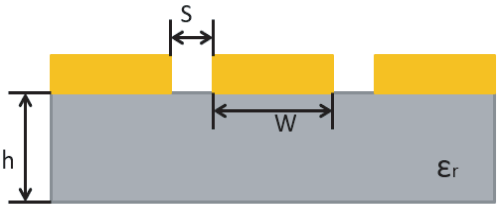

Figure 2. Coplanar waveguide used in the implementation of THz sensor arrays.

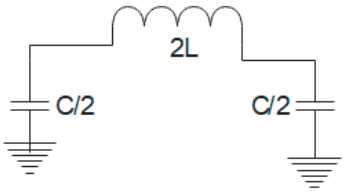

Figure 3. Equivalent circuit for coplanar waveguide.

In Eqs. (1)–(2), Z_o is the characteristic impedance, and ε_e is the effective permittivity of the coplanar waveguide. Z_o and ε_e are given in Equations (3) and (4). Total capacitance and inductance are found by multiplying transmission line length with per unit length capacitance and inductance, respectively.

$$Z_o = \frac{30\pi}{\sqrt{\varepsilon}_e}\frac{K(k)}{K(k')} \tag{3a}$$

$$\varepsilon_e = 1 + \frac{\varepsilon_r - 1}{2}\frac{K(k')}{K(k)}\frac{K(k_1)}{K(k_1')} \tag{3b}$$

In Eqs. (3a) and (3b),

$$k = \frac{a}{b}, \quad k_1 = \frac{\sinh\left(\frac{\pi a}{2h}\right)}{\sinh\left(\frac{\pi b}{2h}\right)}, \quad k' = \sqrt{1-k^2} \tag{4a}$$

$$a = \frac{S}{2}, \quad b = \frac{S}{2} + w \tag{4b}$$

where s is the strip width, and w is the space between strips. K represents a complete elliptical function of the first kind, and K' is its complementary which is defined in Eq. (5).

$$\frac{K(k)}{K'(k)} = \begin{cases} \left[\frac{1}{\pi}\ln\left(2\frac{1+\sqrt{k'}}{1-\sqrt{k'}}\right)\right]^{-1} & \text{for} \quad 0 \leq k \leq 0.7 \\ \frac{1}{\pi}\ln\left(2\frac{1+\sqrt{k}}{1-\sqrt{k}}\right) & \text{for} \quad 0.7 \leq k \leq 1 \end{cases} \tag{5}$$

2.2. Formulation of Split Ring Resonator

Every split ring resonator can be represented as an LC resonator circuit. The ring itself has a self-inductance designated by L_T. The total capacitance can be considered as a parallel combination of gap capacitance, Cg, and inner space capacitance of the ring, Co, as shown in Figure 4.

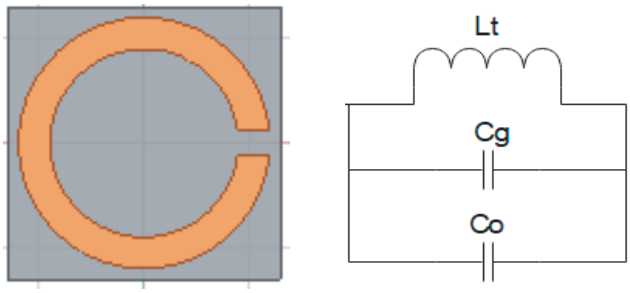

Figure 4. Split Ring Resonator structure and it's equivalent circuit.

Self-inductance can be calculated from the closed ring formulation given in [10, 11] excluding the gap.

$$L_r = 0.002\left(\ln\frac{4l}{c} - \gamma\right)\mu H \tag{6}$$

In Eq. (6), γ is a constant and equal to $\gamma = 2.451$. l is considered to be the length of the ring. The total equivalent capacitance is equal to

$$C_r = C_g + C_o = \varepsilon_o\frac{ct}{g} + \left(\pi\left(r_{ext} - \frac{c}{2}\right) - \frac{g}{2}\right) \times C_{pul} \tag{7}$$

Here r_{ext} is the external radius of the ring, c the ring width, and g the gap for the ring. C_{pul} is calculated using Equation (1) with the characteristic impedance Z_{oSRR} defined in Equation (8). SRR is considered as a coplanar strip here.

$$Z_o = \frac{120\pi}{\sqrt{\varepsilon_e}}\frac{K(k)}{K(k')} \tag{8}$$

The resonant frequency of the SRR can be obtained from,

$$\omega_0 = \frac{1}{\sqrt{L_r C_r}} \tag{9}$$

3. CIRCUIT MODEL AND FORMULATION OF NETWORK PARAMETERS

3.1. Equivalent Circuit Model

The proposed equivalent lumped element circuit for the unit cell, formed with CPW and SRR shown in Figure 1, is given in Figure 5. In the proposed equivalent circuit model, the magnetic wall concept given in [9] is implemented. The mutual coupling between transmission line and SRR is illustrated by M in Figure 5. Mutual inductance between intra unit cell resonators in an array structure is expressed by M'. This is because resonators are inductively coupled, so they will have an additive mutual inductance.

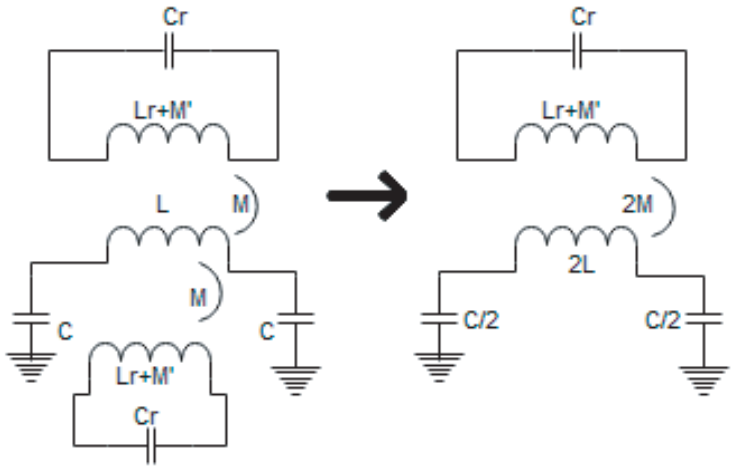

Figure 5. Resultant circuit model with implementation of magnetic wall concept to T-network.

3.2. Transmission Matrix

The unit cell shown in Figure 1 is implemented as a two-port network as shown in Figure 6 and analysed to obtain its network parameters. Periodic structure then can be formed by cascading two port unit cells, and overall network parameters of the array are calculated via $ABCD$ parameters. $ABCD$ parameters of each unit cell are obtained and given by,

$$A = 1 - \frac{\omega C\left[\omega^3 C_r\left\{2L\left(L_r + M'\right) - 4M^2\right\} - 2\omega L\right]}{4\left[\omega^2 C_r\left(L_r + M'\right) - 1\right]} \tag{10a}$$

$$B = \frac{\left[\omega^3 C_r\left\{2L\left(L_r + M'\right) - 4M^2\right\} - 2\omega L\right]}{\left[\omega^2 C_r\left(L_r + M'\right) - 1\right]} \tag{10b}$$

$$C = j\frac{\omega C}{2} - \frac{\omega^2 C^2\left[\omega^3 C_r\left\{2L\left(L_r + M'\right) - 4M^2\right\} - 2\omega L\right]}{16\left[\omega^2 C_r\left(L_r + M'\right) - 1\right]} \tag{10c}$$

$$D = 1 - \frac{\omega C\left[\omega^3 C_r\left\{2L\left(L_r + M'\right) - 4M^2\right\} - 2\omega L\right]}{4\left[\omega^2 C_r\left(L_r + M'\right) - 1\right]} \tag{10d}$$

In Eq. (10), L_r and C_r are the split ring resonator self-inductance and capacitance, respectively. When n number of unit-cells are cascaded together, the $ABCD$ parameters of the overall network are found from,

$$ABCD_{cascade} = ABCD_1 \times ABCD_2 \ldots \times ABCD_n \tag{11}$$

4. MUTUAL INDUCTANCE CALCULATION

In the proposed method, the accurate equivalent circuit model including the effects of complete mutual inductances M and M' is obtained. With Equations (12)–(15), the equivalent circuit in Figure 5 can be transformed as Figure 7 [7], and M can be found.

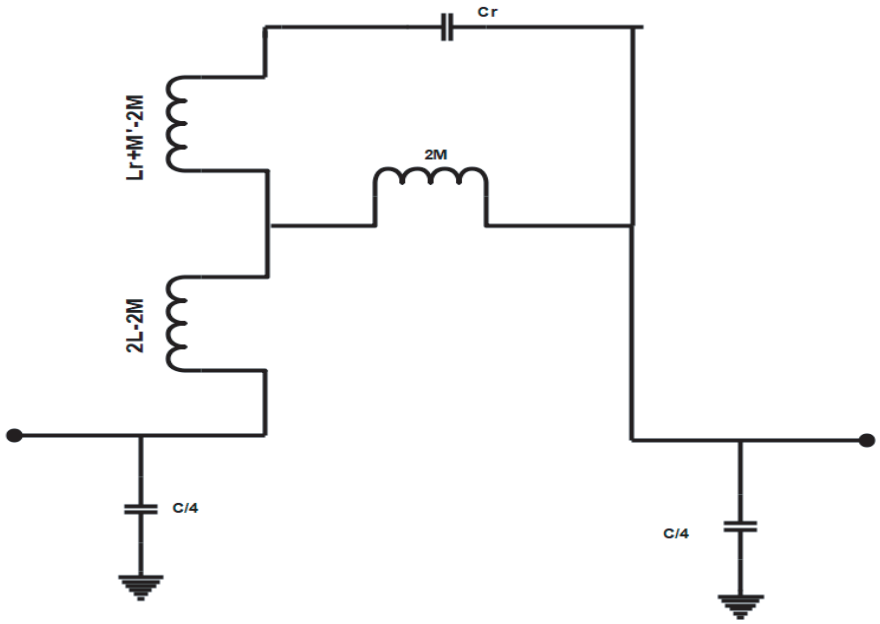

Figure 6. Simplified equivalent two port unit cell network.

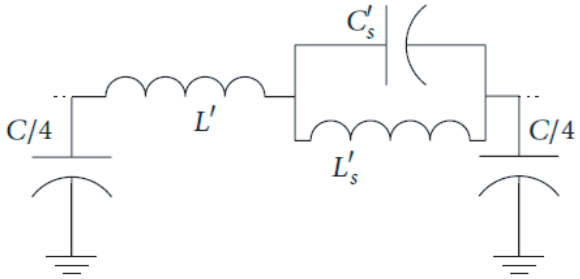

Figure 7. Simplified model without inter resonator mutual inductance.

Resonant frequency of the total structure is expressed as ω_s, and shifted resonant frequency of the resonator itself is denoted as ω_z. Resonant frequency of SRR is shifted from the intrinsic frequency ω_o due to inter ring mutual inductance M'. ω_s and ω_z can be found by EM simulation of the unit cell shown in Figure 1 using S_{11} and S_{21}, respectively.

$$\omega_z = \frac{1}{\sqrt{L'_s C'_s}} \tag{12}$$

where

$$C'_s = \frac{L_r}{4M^2\omega_o^2} \tag{13}$$

$$L_s = 4M^2 C_r \omega_o^2 \tag{14}$$

$$M = \sqrt{\frac{L_s}{4C'_s\omega_o^2}} \tag{15}$$

$$C'_s = \frac{1}{2L}\left[\frac{1}{\omega_s^2 \sim \omega_z^2} + \frac{1}{\omega_z^2}\right] \tag{16}$$

$$M = \sqrt{\frac{L_s}{4C'_s\omega_o^2}} \tag{17}$$

Relation of shifted and intrinsic frequency of SRR gives the inter-ring resonant frequency M'.

$$\omega_z = \frac{\omega_0}{\sqrt{1+\frac{M'}{L_s}}} \tag{18}$$

This method used previously in literature requires the use of 3D EM simulator to estimate mutual inductances. We developed polynomial to find mutual inductance coefficient and ease the design process. Mutual inductance between two inductors valued L_1 and L_2 is found from

$$M = k\sqrt{L_1 \times L_2} \tag{19}$$

Mutual inductance coefficient k in Eq. (16) is obtained using EM simulator by varying critical structural parameters such as substrate permittivity and thickness. The fourth order equation for the mutual inductance, when it is a function of substrate permittivity, is obtained via polynomial curve fitting as shown in Figure 8(a) and given by Equation (20). The coefficients of Equation (20) are illustrated in Table 1 when the substrate thickness is 50 mils. The equation for the mutual inductance is obtained when substrate relative permittivity is varied up to 11.

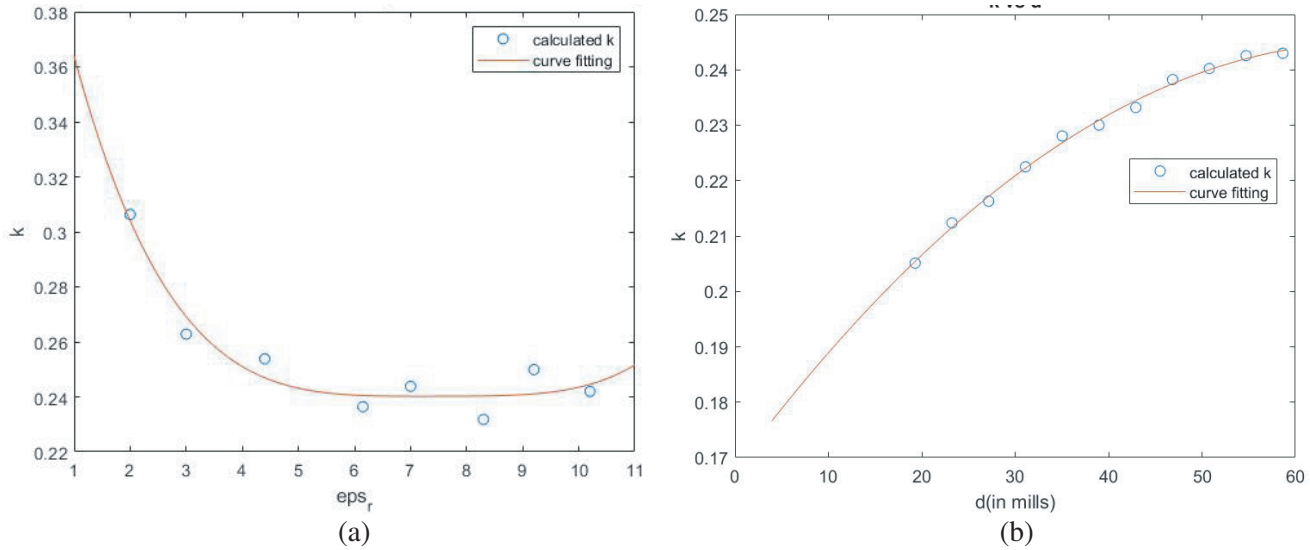

Figure 8. Coupling coefficient as a function of (a) permittivity, and (b) thickness.

Table 1. Fourth order equation coefficient for k as a function of ε_r.

Coefficient	Value
c_1	6.8376×10^{-5}
c_2	-0.0020
c_3	0.0231
c_4	0.1158
c_5	0.4587

$$k(\varepsilon_r) = c_1\varepsilon_r^4 + c_2\varepsilon_r^3 + c_3\varepsilon_r^2 + c_4\varepsilon_r + c_5 \tag{20}$$

The mutual inductance coefficient k is also obtained as a function of substrate thickness, d, via curve fitting as illustrated in Figure 8(b) and given by Equation (21). The coefficients of Equation (21) are given in Table 2 when the relative permittivity of the material, ε_r, is 10.2. Hence, the closed form

Table 2. Second order equation coefficient for k as a function of substrate thickness d.

Coefficient	Value
c_1	-1.66642×10^{-5}
c_2	0.0023
c_3	0.1679

relations for the mutual inductance coefficients are now obtained and given by Equations (20) and (21) which can be used to calculate the mutual inductance of the structure given by Eq. (19).

$$k(d) = c_1 d^2 + c_2 d + c_3 \tag{21}$$

5. SIMULATION AND MEASUREMENT RESULTS

The resonator unit cell formed with SRR and CPW transmission lines shown in Figure 1 is simulated using 3D EM simulator and compared with the simulation results using nonlinear circuit simulator ADS for the proposed lumped element equivalent circuit model given in Figure 5. The results are then compared with the analytical results and illustrated in Figure 9.

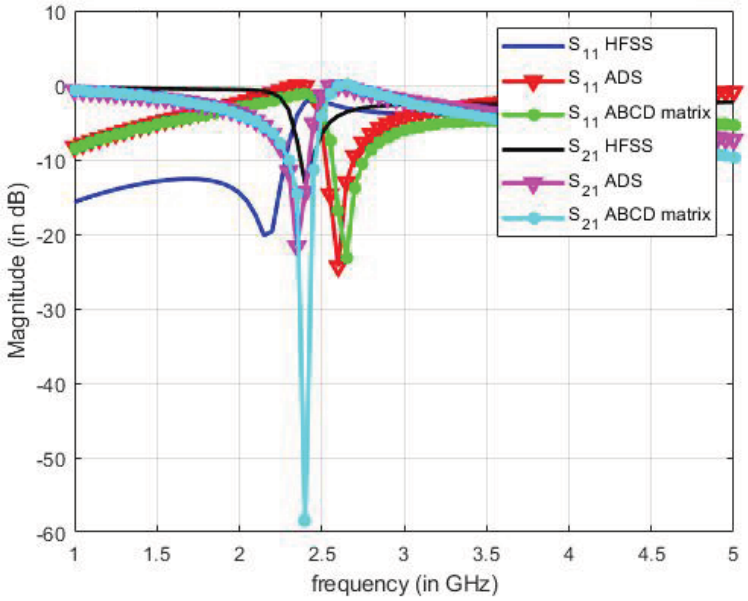

Figure 9. Comparison of analytical results with ADS and HFSS when Copper ring radius = 2.69 mm, ring width = 0.4 mm, gap = 0.1 mm, ring thickness = 17.5 µm, substrate thickness = 1.27 mm, CPW strip width, $W = 8$ mm, Slot width, $S = 1.43$ mm, line length, $l = 6$ mm for ROGER3210 ($\varepsilon_r = 10.2$).

It has been observed in Figure 9 that the resonant frequency based on S_{21} matches between analytical and simulation results. However, the simulation results of ADS and analytical results are slightly shifted from the results obtained using HFSS. The slight deviation is due to the effect of the mutual inductance.

The proposed method is implemented also at the THz range, and simulation results are given in Figure 10.

The prototype of the unit cell given in Figure 1 is built and measured as shown in Figure 11. The simulation and measurement results are given in Figure 12(a) and Figure 12(b). The slight shift in

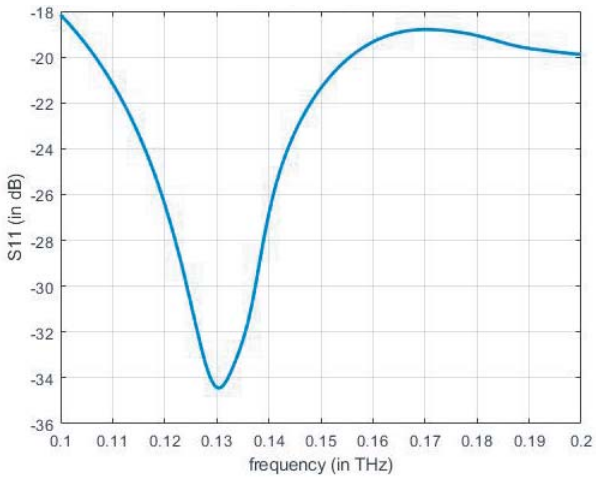

Figure 10. THz Simulation Copper ring radius = 30 µm, ring width = 6 µm, gap = 2 µm, ring thickness = 200 nm, substrate thickness = 1 mm, CPW strip width, W = 150 µm, Slot width, S = 90 µm, line length, l = 300 µm and substrate is Silicon (ε_r= 11.9).

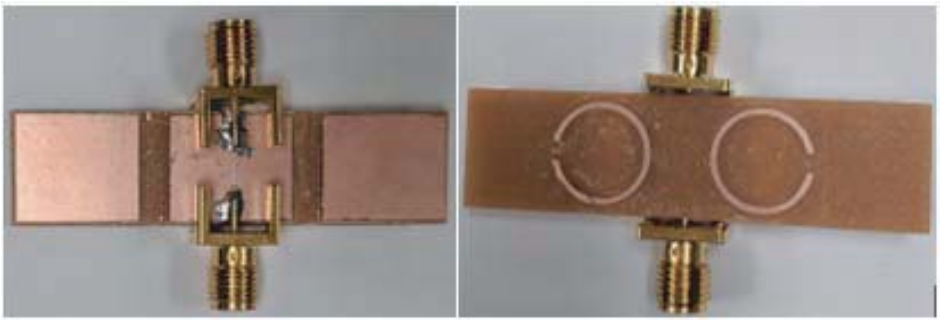

Figure 11. The prototype of the metamaterial transmission line unit cell.

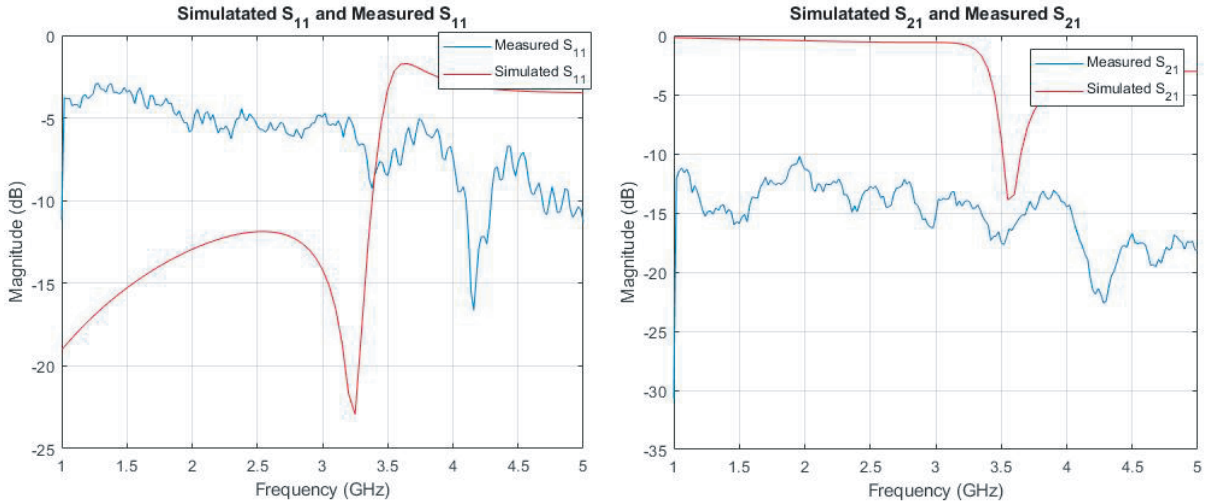

Figure 12. Comparison of Simulation and Measurement of (a) S_{11} and (b) S_{21} for Copper ring radius = 4.8 mm, ring width = 0.8 mm, gap = 2.5 mm, ring thickness = 17.5 µm, substrate thickness = 1.5 mm, CPW strip width, W = 15 mm, Slot width, S = 3.5 mm, line length, l = 13 mm and substrate is FR4 (ε_r = 4.4).

the resonant frequency is observed between simulated and measured results for both S_{11} and S_{21}. The deviation is due to mutual inductance and the effect of imperfect port impedance in the prototype. Overall, the results are found in agreement as shown in Figure 11 with a small deviation in the resonant frequency.

6. CONCLUSION

In this paper, the complete formulation of THz sensor array which is formed with SRR and CPW is given using network parameter method in conjunction with curve fitting using 3D EM simulator. The proposed equivalent circuit model is simple and can be used to obtain the network parameters of the complete array system with ease. Furthermore, the proposed method takes into consideration of the full mutual inductance effect existing in the resonator structure. The analytical method proposed in this paper is compared with 3D EM and circuit simulation results, and agreement is observed on all of them. The prototype is then built and measured. It has been shown that the measurement results are in agreement with simulated and analytical results.

REFERENCES

1. Veselago, V., "The electrodynamics of substances with simultaneously negative values of permittivity and permeability," *Usp. Fiz. Nauk*, Vol. 92, 517, 1967.
2. Pendry, J. B., A. Holden, W. Stewart, and I. Youngs, "Extremely low frequency plasmons in metallic mesostructures," *Physical Review Letters*, Vol. 76, No. 25, 4773, 1996.
3. Pendry, J. B., A. J. Holden, D. J. Robbins, and W. Stewart, "Magnetism from conductors and enhanced nonlinear phenomena," *IEEE Transactions on Microwave Theory Techniques*, Vol. 47, No. 11, 2075–2084, 1999.
4. Yen, T.-J., et al., "Terahertz magnetic response from artificial materials," *Science*, Vol. 303, No. 5663, 1494–1496, 2004.
5. Smith, D. R., W. J. Padilla, D. Vier, S. C. Nemat-Nasser, and S. Schultz, "Composite medium with simultaneously negative permeability and permittivity," *Physical Review Letters*, Vol. 84, No. 18, 4184, 2000.
6. Martın, F., J. Bonache, F. A. Falcone, M. Sorolla, and R. Marqués, "Split ring resonator-based left-handed coplanar waveguide," *Applied Physics Letters*, Vol. 83, No. 22, 4652–4654, 2003.
7. Aznar, F., et al., "Characterization of miniaturized metamaterial resonators coupled to planar transmission lines through parameter extraction," *Journal of Applied Physics*, Vol. 104, No. 11, 114501, 2008.
8. Naqui, J., A. Fernández-Prieto, F. Mesa, F. Medina, and F. Martín, "Effects of inter-resonator coupling in split ring resonator loaded metamaterial transmission lines," *Journal of Applied Physics*, Vol. 115, No. 19, 194903, 2014.
9. Naqui, J., L. Su, J. Mata, and F. Martín, "Recent advances in the modeling of transmission lines loaded with split ring resonators," *International Journal of Antennas Propagation*, Vol. 13, 1–13, 2015.
10. Eroglu, A., *RF Circuit Design Techniques for MF-UHF Applications*, CRC Press, 2016.
11. Greenhouse, H., "Design of planar rectangular microelectronic inductors," *IEEE Transactions on Parts, Hybrids, Packaging*, Vol. 10, No. 2, 101–109, 1974.